The Canadian Society for Bioengineering
The Canadian society for engineering in agricultural, food, environmental, and biological systems.

CSBE | SCGAB

La Société Canadienne de Génie Agroalimentaire et de Bioingénierie
La société canadienne de génie agroalimentaire, de la bioingénierie et de l'environnement

Paper No. 06-124

SELECTION AND TESTING OF SPECTRAL BANDS FOR EDGE-BASED LEAF SEGMENTATION

Scott D. Noble

University of Lethbridge, 4401 University Drive, Lethbridge, AB T1K 3M4.
scott.noble2@uleth.ca

Ralph B. Brown

University of Guelph School of Engineering, Guelph, ON N1G 2W1

Written for presentation at the
CSBE/SCGAB 2006 Annual Conference
Edmonton Alberta
July 16 - 19, 2006

Abstract

Leaf shape is an important feature used in plant identification. The first step in automating leaf shape analysis in complex, real-world scenes is to segment individual leaves. Leaves are often occluded and overlapping, and the similar colour and texture characteristics of the leaves complicate the task of separating them. A segmentation approach based on simple edge detectors operating on narrow-waveband images from an imaging spectrophotometer was developed and tested. Band selection was done by comparing separability of leaf-leaf, vein, and leaf-overlap edge regions of multi-plant, images for four species in 115 spectral bands between 400 and 1000 nm. Testing resulted in a mean segmentation percentage of 63% using a Sobel edge detector operating on an image in a 5 nm waveband centred at 719 nm. This result compared favourably with existing research given the relative simplicity of the segmentation algorithm and complexity of the test images used.

Keywords: segmentation, hyperspectral imaging, edge detection, band selection

SELECTION AND TESTING OF SPECTRAL BANDS FOR EDGE-BASED LEAF SEGMENTATION

Scott D. Noble[1], Ralph B. Brown[2]

Abstract: Leaf shape is an important feature used in plant identification. The first step in automating leaf shape analysis in complex, real-world scenes is to segment individual leaves. Leaves are often occluded and overlapped, and the similar colour and texture characteristics of the leaves complicate the task of separating them. A segmentation approach based on simple edge detectors operating on narrow-waveband images from an imaging spectrophotometer was developed and tested. Band selection was done by comparing separability of leaf-leaf, vein, and leaf-overlap edge regions of multi-plant, images for four species in 115 spectral bands between 400 and 1000 nm. Testing resulted in a mean segmentation percentage of 63% using a Sobel edge detector operating on an image in a 5 nm wide waveband centred at 719 nm. This result compared favourably with existing research given the relative simplicity of the segmentation algorithm and complexity of the test images used.

Keywords: segmentation, hyperspectral imaging, edge detection, band selection

While the spectral features of plants have been studied in the context of automated plant identification, they have very little heritage within manual plant identification systems. Even colour is used sparingly, generally reserved for flowers or seeds. Shape features stand in contrast; the shapes of leaves, seeds, and to a lesser degree entire plants, are common elements of traditional plant taxonomies. Despite these established methods for identification, incorporating these shape features into automated systems has proven difficult. One reason for this is the challenge of separating individual green leaves out of an image containing other similar green leaves. Segmentation of leaves in the image is a necessary precursor to the use of leaf shape in automated identification. There are a number of solutions that take advantage of the spectral signature of green plant tissues when individual leaves are set entirely against a non-plant background. The difficulty arises when individual leaves overlap and occlude one another. Differences between individual leaves can be subtle, making the boundaries between them difficult to define and creating a significant challenge for subsequent shape analysis.

In this study, an approach to leaf segmentation was investigated that took advantage of the NIR wavebands for separating leaves from one another and explored the utility of classical edge detectors for defining leaf-leaf boundaries.

Paper No. 06-124, presented at the CSBE/SCGAB 2006 Annual Conference, Edmonton, AB. July 16-19, 2006.
[1]Corresponding Author. University of Lethbridge, Lethbridge, AB T1K 3M4. scott.noble2@uleth.ca. [2]School of Engineering, University of Guelph, Guelph, ON.

Background

Segmentation for shape identification may refer to separating an entire plant from the background for plant-scale shape features, or separating individual leaves from the rest of the plant. Separating the entire plant may be done using a number of spectral and colour based approaches. Where possible, the use of NIR information improves the plant/background segmentation due to the large reflectance differences in this region. NIR information was used by Guyer et al. (1986) via a NIR sensitive camera, and Guyer et al. (1993) using a camera and visible blocking filter. As digital RGB cameras have become readily available (and NIR bands have not), segmentation approaches using colour indices have been more common. A modified excess green measure (2g-r-b) using the normalized chromacity values, has been used to good effect (Woebbecke et al. 1995; Tang et al. 2003) to segment plants. A study by Philipp and Rath (2002) on using colour space transformations for plant discrimination found that the third component of the i1i2i3 colour space, and of their modified $i1i2i3_{new}$ colour space were better than other colour space transforms investigated. On closer examination, the i3 component of the i1i2i3 space was essentially equivalent to the modified excess green measure, with the $i3_{new}$ being only slightly different.

Until plants reach a point where individual plants are starting to overlap each other, the entire plant approach may be appropriate. However, as scene complexity increases and individual leaves are required, these approaches are hindered by the similarity of leaf colour. Some work has been done on this problem. Lee and Slaughter (2004) developed a watershed-style algorithm for defining boundaries between multiple-leaf blobs that had been segmented from a colour image. This approach attained up to 57% separation performance on tomato seedlings, with this measure defined as the number of properly segmented leaves divided by the sum of leaves that were fragmented, not separated, and separated. It was, however, computationally demanding.

Deformable templates have also been investigated for leaf segmentation (Manh et al., 2001). Green foxtail (SETVI) and background were segmented using colour information. Starting points for template fitting were defined as leaf tips, which were found using a global search by a small window, followed by regional assessment when the small window was covering plant pixels exclusively. An ellipse was rotated around the tip, and the position that yielded the highest number of plant pixels covered by the ellipse was taken as the template starting point. The template was iteratively deformed outward until a stopping criterion was met. This approach was somewhat dependent on leaves having definable tips, the appropriate definition of the template skeleton, and was not able to account for shared leaf edges within the term driving the deformation, making it somewhat susceptible to occlusion. As such, it does not appear to be a globally applicable solution.

An edge-following algorithm was developed by Franz et al. (1995) for use with broadband NIR plant images. After determining gradient slope and magnitude using a set of 3x3 Sobel kernels, edges were traced using a series of algorithms that were similar to those of the Canny edge detector (Trucco and Verri, 1998 pg 71-79) but with a considerable amount of additional logic for excluding petioles and stems and for linking edges. Leaf extraction rates for the four species studied ranged from 71.4% for giant foxtail (SETFA) to 95.8% for ivyleaf morning glory (IPOHE). The algorithms developed required significant user input for deciding where to start traces and locating areas of interest, but demonstrated the potential of using NIR information, in which there can be considerable variation between leaves, and edge-based segmentation for leaf separation.

One of the challenges in using edge-based approaches to segmentation of leaves is the large degree of variation of edge strengths within the regions of interest. The edge strength between leaf and soil are very large, while leaf-to-leaf edge strengths are lower. Leaf veins and texture also add edge components to the image. Images need to have high edge strength contrast between overlapping leaves relative to other internal edges, which is not typical in RGB images. A possible simplification of the edge-based approach could be made if leaf edges were strong enough relative to other edges to be found continuously around the leaf, even in areas of occlusion (leaf-leaf boundary). In this case, the edge-strength image could be thresholded at this level and simply subtracted from the vegetation image mask. By subtracting the leaf edges, the leaf interiors would be separated from one another, leaving an image of blobs which could be further analyzed for shape.

Objectives

Given the degree of variation observed between leaves in the NIR bands of the hyperspectral imagery available, it was hypothesised that a band would exist with sufficient contrast between leaves to make edge-subtraction segmentation feasible. Since edges occurring at the boundary between green vegetation and the background are both very strong and easily obtained from the vegetation mask, only the interior edges were of interest for band selection. Interior edges could be due to leaf-leaf boundaries (leaf overlap), veins, or blemishes on a leaf. The first objective was to identify a waveband at which leaf-leaf boundaries were differentiable from other interior edges. This band would then be used to test the edge-subtraction segmentation approach using the edge-strength image from a Sobel edge enhancer, and from a Canny edge detector, the algorithm of which has some commonalities to the algorithm used by Franz et al. (1995).

Methods

Spectral images were collected of trays containing several specimens of four plant species using the University of Saskatchewan imaging spectro-photometer (Noble et al. 2003; Noble 2006). For each tray, the data cube contained data in 115 spectral bands between 400 and 1000 nm at five nanometre bandwidths and intervals. The four species selected were redroot pigweed (*Amaranthus retroflexus*, AMARE), common purslane (*Portulaca oleracea*, POROL), soybean (*Glycene max* sp., SOYBE), and stinkweed (aka field pennycress, *Thlaspi arvense*, THLAR). These species represented a range of leaf properties (venation, thickness, size) and plant growth patterns. One maturity level for each species was chosen, and the entire-tray image was used for each.

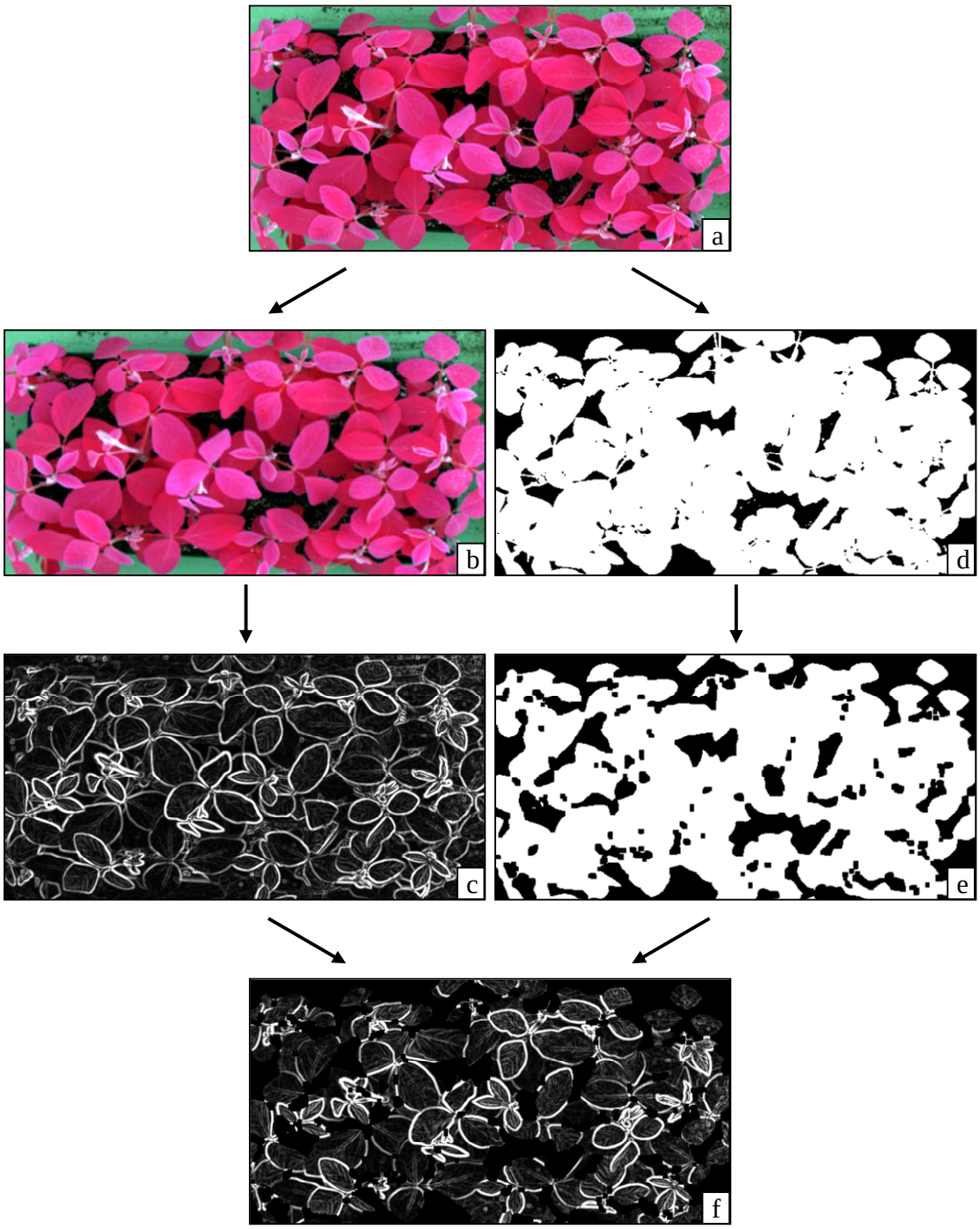

Figure 1. Example of processing steps for interior edge extraction: (a) false-colour composite of original image, (b) image 'a' after Gaussian smoothing, (c) edge image of 'b', (d) vegetation mask of image 'a,' (e) two erosion iterations of image 'd', (f) image 'c' multiplied by image 'e'.

The vegetation mask image was created for segmenting plant material from the background, taking advantage of the change in reflectance between the red and NIR portions of the spectrum. The vegetation mask was in represented as a binary image, and calculated according to equation 1:

$$Vmask(\mathbf{x}) = \left(\frac{R_{760}(\mathbf{x})}{R_{667}(\mathbf{x})} > 3 \right) \wedge (R_{760}(\mathbf{x}) > 30\%), \quad \textbf{(1)}$$

where $\boldsymbol{x}$ is the location vector for the images, and R_{760} and R_{667} are the image bands at 760 and 667 nm, respectively.

Edge-strength images were generated for each datacube by first smoothing each band with a 5 x 5 Gaussian kernel, followed by a pair of 3 x 3 Sobel kernels. The edge-strength image was the sum of outputs from the horizontal and vertical Sobel convolutions (ENVI Sobel operator, Research Systems Inc., Boulder, CO). As only the interior leaf edges were of interest for band selection, the exterior (plant-background) edges were removed by masking the edge-strength images with a two-iteration erosion version of their vegetation masks. An example of these operations and a resulting interior edge-strength image are shown in Figure 1.

For each species, sample points were selected at interior boundaries. Where possible, three leaf-leaf overlap edges categories were used: overlap involving new and old leaves, overlap of leaves high in the canopy over lower leaves, and overlap of peer leaves. Peer leaves were leaves of similar maturity, reflectance, and height within the canopy. Edge categories that did not represent leaf boundaries were veins, general leaf tissue, and overlap bleedthrough. Bleedthrough occurred in some instances where the outline of an occluded leaf was visible through the covering leaf. Basic descriptive statistics of edge strength were calculated for each edge class in all wavebands, and the Fisher criterion calculated for all interior leaf edge versus non-leaf edge combinations:

$$Fisher = \frac{(\overline{X_1} - \overline{X_2})^2}{s_1^2 + s_2^2}, \qquad \textbf{(2)}$$

where $\overline{X_i}$ is the mean of class *i*, and s_i^2 is the variance of class *i*.

Class means and the minimum Fisher criterion at each waveband were plotted (Figure 2). Candidate bands were selected based on the Fisher criterion plots and observation of animations of the edge-strength bands. The performances of the selected wavebands were compared by plotting the edge strengths along transects of the images, and a band selected based on these comparisons.

Edge-based segmentation was tested for the Canny and Sobel edge detectors using the selected band. The Canny edge detector was implemented in IDL (Research Systems Inc., Boulder, CO, while the Sobel detector was a built-in function of IDL. Tests were conducted on a window around the previously defined transects. The image was masked by the vegetation mask and the edge detectors were applied. Threshold values were set using the edge transects and testing. The vegetation mask was then masked by the inverse of the thresholded edge images (edges = 0, everything else = 1). These results went through a single iteration of the NI-IMAQ Separation operator (National Instruments, Austin TX) to remove small isthmuses joining neighbouring blobs, followed by a particle filter to remove all blobs smaller than 30 pixels. A hole-filling operation was done to fill interior holes in the leaf blobs left by wholly interior vein edges. Lastly, the segmented leaf image was opened (erosion followed by dilation) to smooth the leaf blob boundaries. Results of the Canny and Sobel based segmentation schemes were compared by counting the number of leaves fully or partially visible in the original image. The number of correctly segmented leaves, un-segmented leaves, and over-separated leaves were counted in each of the segmented images. Comparisons were made based on the rates of segmentation, un-segmentation, and removal.

Results and discussion

Mean edge strengths and Fisher criterion values for the four sample species are shown in Figure 2. The pattern of edge strengths corresponded closely to the typical patterns of leaf reflectance and degree of difference between leaves. All species showed separability in the red edge region based on the Fisher criterion, with all but SOYBE reaching a global maximum there. The red edge location is sensitive to variations in chlorophyll content, which is influenced in turn by leaf maturity and light exposure. The global maximum for SOYBE was at 745 nm, which is at the upper end of the red edge region. Local maxima were located around 552 nm for all species. Low Fisher criterion values were found for AMARE, and to a lesser extent THLAR. These species both showed significant bleedthrough effects in the NIR bands, with the edge of occluded leaves being clearly visible through the covering leaves in several cases. For the purposes of this study, these were interpreted as false edges. In the case of the new-old and bleedthrough classes for AMARE, mean edge strengths were nearly identical from 800 to 1000 nm, and were greater than the peer-peer edge strengths from 735 to 1000 nm.

Wavebands centred at 714, 719, and 745 nm were selected for further analysis on the basis of being the locations of global maximum Fisher criterion value for one or more of the sample species. The band centred on 552 nm was included as a means of comparing NIR performance with what might be possible with visible information only. An additional band, centred at 823 nm was also included. This band appeared to have good interior leaf edge enhancement and non-leaf-edge suppression characteristics when the bands of the SOYBE sample were viewed as an animation.

A transect line was drawn across each sample

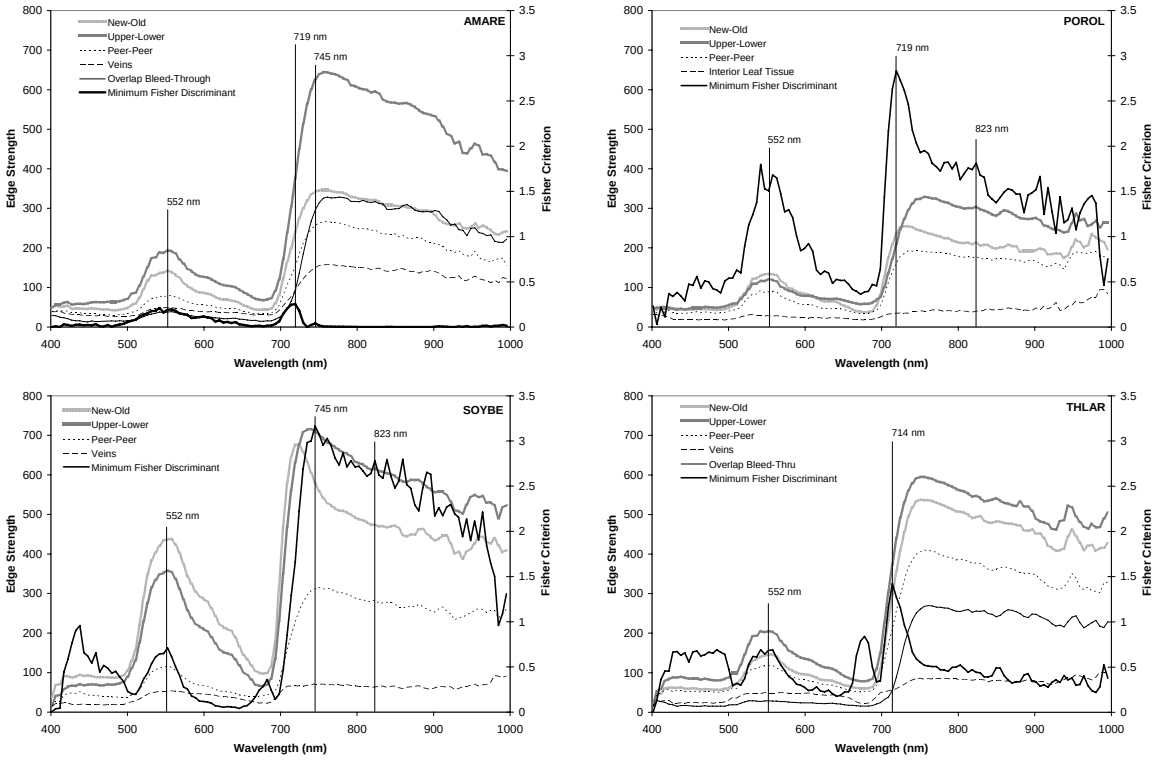

Figure 2 Interior edge class means (primary axis) and the minimum pairwise Fisher criterion for leaf versus non-leaf edge (secondary axis) for AMARE, POROL, SOYBE and THLAR.

species datacube. This line was positioned with the intent of crossing as many of the different edge classes as possible. The edge strengths along the transect lines were plotted for each of five candidate bands, and arranged below a corresponding false-colour composite image of the transect line and surrounding area. Vertical lines were drawn through the plots at points where the transect line intersected an edge. Solid lines were placed at leaf boundaries and dashed lines were placed at veins or other undesired edges. In some cases, edges appeared along leaf-background boundaries, even after these had been removed or reduced. These edges were ignored. In general, leaf boundary edge strengths increased with wavelength. Background-noise edge strength also increased in some instances. Edge strengths and the response of edges caused by veins with respect to wavelength varied with species.

Leaf-boundary edges of AMARE (Figure 3) were the most difficult to clearly separate from non-leaf boundary edges. While the strength of leaf-boundary edges tended to increase with wavelength, non-boundary edges caused by veins and bleedthrough often did as well. Edge strengths were also generally lower than some of the other species. Based on these observations, 714 and 719 nm were identified as the best candidate bands for edge-based segmentation of AMARE. The edge strength of bleedthrough and vein features increased substantially in the bands with longer wavelengths.

Analysis of the POROL edge transect was inhibited somewhat by the small leaf size and corresponding high number of leaf boundaries. Bleedthrough edges were not evident with POROL, possibly due to leaves being thicker and better diffusers of light. Veins were not visible. Edge strengths increased with wavelength until 745 nm, decreasing or remaining approximately the same at 823 nm. Wavebands centred at 719 and 745 nm were selected as the best candidates for separating POROL leaf boundaries.

The edges of the SOYBE transect were generally the strongest and most clearly defined of the four species. Unlike AMARE, vein edges were most pronounced at shorter wavelengths, diminishing to near zero at 745 and 823 nm. However, the one instance of a bleedthrough edge in the transect increased in strength at these same wavelengths. The wavebands at 719 and 745 nm were selected as potential bands based on the SOYBE sample.

Bleedthrough effects were very evident in the THLAR sample, thought not well represented in the transect. The bleedthrough edge became relatively pronounced at 745 and 823 nm, while being unperceivable in the visible and faint in the other NIR bands. Edges due to veins were insignificant in the

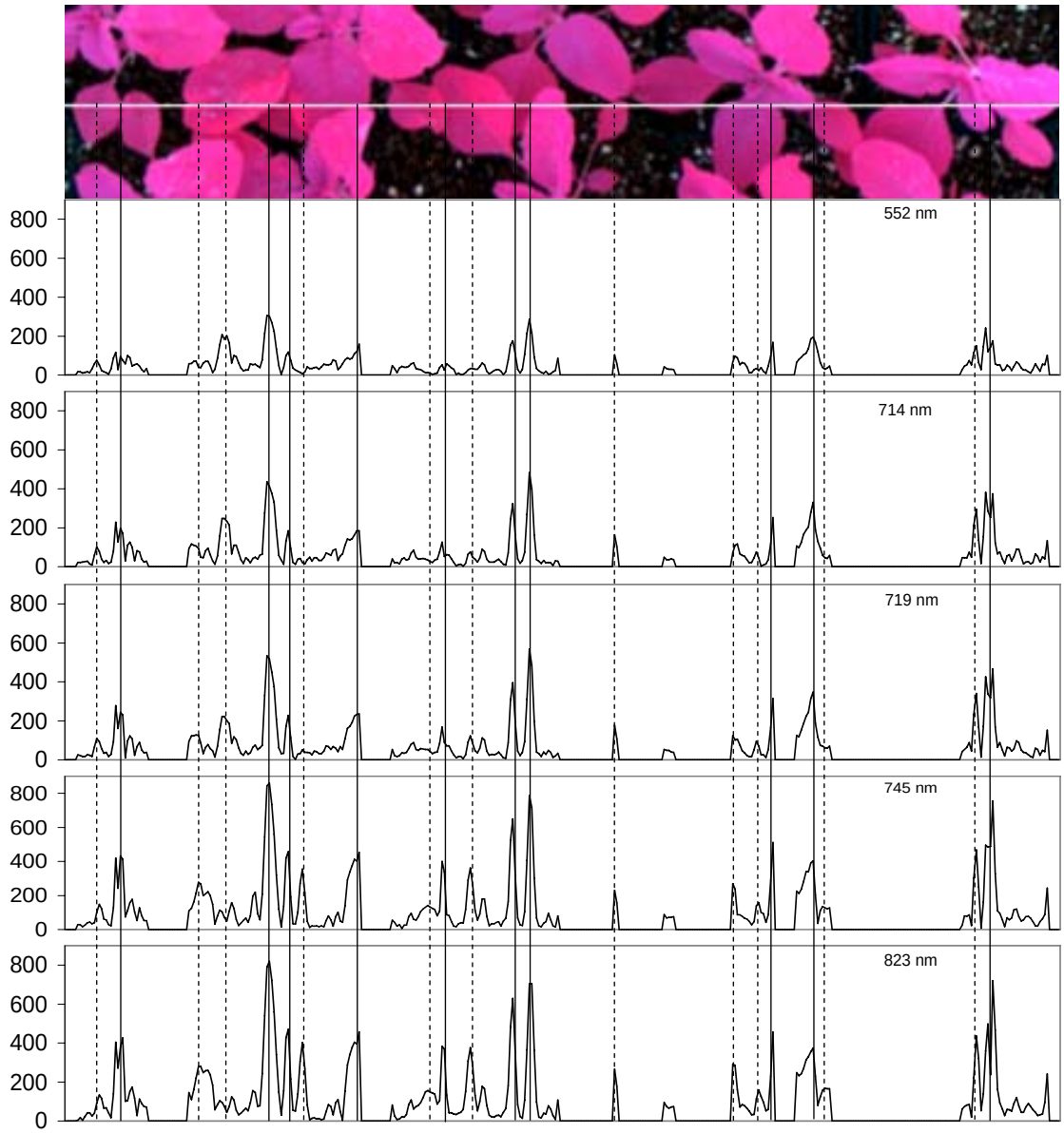

Figure 3 Edge strength transect for AMARE. Solid lines correspond to leaf edges, dashed lines correspond to non-boundary edges.

transect. In an attempt to minimize the bleedthrough effect and maximize leaf boundary edge strength, the band centred at 719 nm was selected as the best candidate band based on the THLAR sample

While not optimum for all of the samples, the band at 719 nm was selected overall for testing the edge-subtraction leaf segmentation approach.

Edge-based segmentation testing

Edge threshold images were determined for each of the four transect-window images. The edge strength threshold was set at 225 for the Sobel-based edges. The Canny edge strength was calculated as the root sum of squares of the horizontal and vertical gradients. Based on test histogram of these edge strengths, the high Canny threshold was set at 30, and the low threshold set at five, with hysteresis search neighbourhood of width five. These images were input into a LabVIEW routine with the corresponding vegetation mask images and the Canny and Sobel-based segmentation images produced. A sample of the transect image, Canny-segmented image, and Sobel-segmented images are shown for THLAR in Figure 4. Several examples of the differences in segmentation are numbered in the Canny and Sobel-based segmentation images.

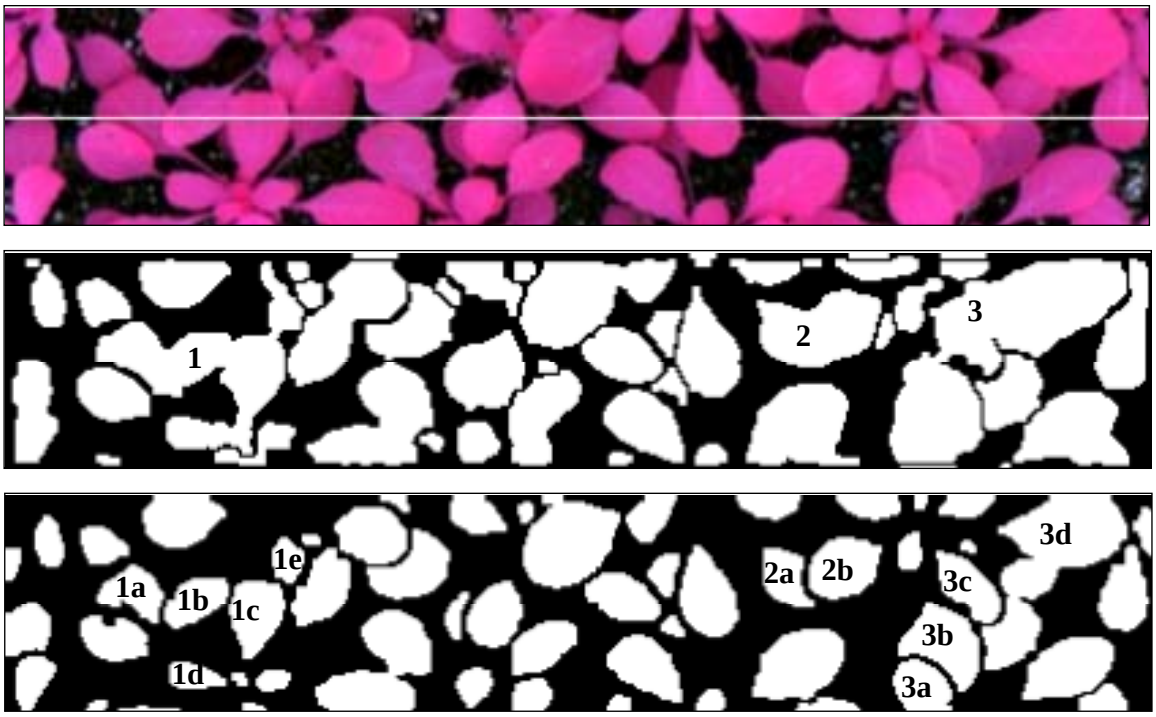

Figure 4 THLAR transect window image (top), with Canny-based segmentation image (middle), and Sobel-based segmentation image (bottom). Numbered blobs in the Canny image are examples of blobs that were not segmented; numbered blobs in the Sobel image are the corresponding blobs more adequately segmented.

Leaves in the transect-window images were manually numbered, and the corresponding blobs in the segmentation images labelled. Segmented blobs that corresponded to a single leaf were counted as correctly segmented; shape correspondence was not a major factor in this labelling. Cases of multiple leaves corresponding to a single blob were counted as un-segmented; each actual leaf within the bounds of these blobs was counted in this total. A set of blobs that corresponded to a single leaf was counted as a split leaf. The number of leaves eliminated for each case was calculated as the difference between the number of leaves identified in the transect window and the sum of segmented, un-segmented, and split leaves. Rates of correctly segmented, un-segmented, and eliminated leaves were calculated by dividing these quantities by the number of leaves in the corresponding transect window. Counts and rates are shown by species and edge-detection scheme in Table 1. Mean rates are shown across species. The Sobel-based segmentation had a higher segmentation rate and a lower un-segmented rate for all four samples. Split numbers and elimination rates were slightly higher for the Sobel-based segmentation. The higher elimination rate is beneficial for further stages of processing, as the leaves that are eliminated are small leaves or occluded leaf segments that add clutter to the segmented leaf image. Generally, the fineness of the edge extracted by the Canny edge detector is one of its main benefits. For image segmentation in this context, however, the relatively wide edges extracted by the Sobel edge enhancer proved better able to segment the leaf blobs.

With a mean segmented fraction of 63%, the performance of the Sobel segmentation scheme is lower than that reported by Franz et al. (1995). However, the test images used in this study contained multiple plants in dense stands as opposed to single

Table 1 Segmentation results.

	Number of Leaves	Fraction Properly Segmented		Fraction Unsegmented		Fraction Eliminated	
		Canny	Sobel	Canny	Sobel	Canny	Sobel
AMARE	49	0.45	0.71	0.49	0.12	0.04	0.12
POROL	113	0.23	0.56	0.79	0.29	-0.02	0.14
SOYBE	66	0.45	0.55	0.50	0.32	0.03	0.06
THLAR	71	0.35	0.72	0.54	0.10	0.10	0.17
Mean		0.37	0.64	0.58	0.21	0.04	0.12

seedlings. The algorithm used by Franz et al. (1995) also had considerable logic in addition to that contained in the standard Canny algorithm, allowing it to both search for weaker edges that were not parallel to main edges above the high threshold, and for estimating occluded edges. This more advanced algorithm comes at significantly higher cost than the Sobel-based edge subtraction approach.

Conclusions

A leaf segmentation approach was tested that used a combination of a vegetation mask and an edge strength image that was calculated for a band that provided contrast for leaf-leaf boundaries. Based on tests with four species, the band centred at 719 nm was selected. Comparisons were made between edges found using a Sobel edge detector and a Canny edge detector. Masking the vegetation binary image with the inverse Sobel edge threshold image resulted in an average correct leaf segmentation rate of 63%. This approach effectively and simply segmented the upper, un-occluded leaves of the image from those underneath. It was not able to reconstruct the occluded leaves, or to specifically eliminate partial leaves from consideration. As such, any shape identification that is run subsequently to this segmentation step must have a mechanism for ignoring partial leaf sections.

A shortcoming of the Sobel segmentation is that it removes a significant amount of the leaf area. This can alter the shape of smaller blobs in particular. It is also highly dependent on the ability of the band selected to provide leaf-leaf edge contrast while minimizing edges from veins and blemishes. It was observed that no single band was optimal for all species, and that veins of different species did not always change in the same way with wavelength. Further study on methods for selecting appropriate bands for this type of operation is warranted.

References

Franz, E., M. R. Gebhardt, and K. B. Unklesbay. 1995. Algorithms for extracting leaf boundary information from digital images of plant foliage. *Transactions of the ASAE*, 38(2): 625-633.

Guyer, D. E., G. E. Miles, M. M. Schreiber, O. R. Mitchell, and V. C. Vanderbilt. 1986. Machine vision and image processing for plant identification. *Transactions of the ASAE*, 29(6): 1500-1507.

Guyer, D. E., G. E. Miles, L. D. Gaultney, and M. M. Schreiber. 1993. Application of machine vision to shape analysis in leaf and plant identification. *Transactions of the ASAE*, 36(1): 163-171.

Lee, W. S., and D. C. Slaughter. 2004. Recognition of partially occluded plant leaves using a modified watershed algorithm. *Transactions of the ASAE*, 47(4): 1269-1280.

Manh, A. G., G. Rabatel, L. Assemat, and M. J. Aldon. 2001. Weed leaf image segmentation by deformable templates. *Journal of Agricultural Engineering Research*, 80(2): 139-146.

Noble, S. D. 2006. "A Framwork for Machine-Vision Based Plant Identification" Ph.D. Thesis, University of Guelph, Guelph, ON. In review.

Noble, S. D., M. Crookshank, and T.G. Crowe. 2003. The design of a ground-based hyperspectral imaging / imaging spectrophotometer system. Paper No. 03-204, *CSAE/SCGR 2003 Meeting*, Montreal, PQ.

Philipp, I., and T. Rath. 2002. Improving plant discrimination in image processing by use of different colour space transformations. *Computers and Electronics in Agriculture*, 35: 1-15.

Tang, L., L. Tian, and B. L. Steward. 2003. Classification of broadleaf and grass weeds using gabor wavelets and an artificial neural network. *Transactions of the ASAE*, 46(4): 1247-1254.

Trucco, E., and A. Verri. 1998. *Introductory techniques for 3-d computer vision.* Upper Saddle River, NJ: Prentice Hall.

Woebbecke, D. M., G. E. Meyer, K. Von Bargen, and D. A. Mortensen. 1995. Color indices for weed identification under various soil, residue, and lighting conditions. *Transactions of the ASAE*, 38(1): 259-269.